Mitotic H3K9ac is controlled by phase-specific activity of HDAC2, HDAC3 and SIRT1

Shashi Gandhi[1], Raizy Mitterhoff[1], Rachel Rapoport[1], Sharon Eden[1], Alon Goran[2] and Itamar Simon[1*]

[1]Department of Microbiology and Molecular Genetics, Institute of Medical Research Israel-Canada, Faculty of Medicine, The Hebrew University, Jerusalem 91120, Israel;

[2] Department of Medicine, University of California, San Diego, La Jolla, California 92093, USA

*Corresponding Author

itamar.simon1@mail.huji.ac.il

Abstract

Mitosis comprises multiple changes, including chromatin condensation and transcription reduction. Intriguingly, while histone acetylation levels are reduced during mitosis, the mechanism of this reduction is unclear. We studied the mitotic regulation of H3K9ac by using inhibitors of histone deacetylases. We evaluated the involvement of the targeted enzymes in regulating H3K9ac during mitotic stages and cytokinesis by immunofluorescence and immunoblots. We identified HDAC2, HDAC3 and SIRT1 as modulators of the mitotic levels of H3K9ac. HDAC2 inhibition increased H3K9ac levels in prophase, whereas HDAC3 or SIRT1 inhibition, increased H3K9ac levels in metaphase. Next, we performed ChIP-seq in mitotic cells following targeted inhibition of these histone deacetylases. While the genomic areas impacted by HDAC2 and HDAC3 were mostly concordant, a subset of loci were unique to each enzyme. Interestingly, HDAC3-specific targets were enriched for genes involved in mitosis regulation. Our results support a model in which H3K9 deacetylation is a stepwise process – at prophase HDAC2 modulates most transcription-associated H3K9ac-marked loci and at metaphase HDAC3 maintains the reduced acetylation, whereas SIRT1 potentially regulates H3K9ac by impacting HAT activity.

Introduction

The eukaryotic cell cycle is composed of many cellular events. During interphase the genome and other cellular components are duplicated, and during mitosis the cell is divided into two daughter cells. The relatively short phase of mitosis is tightly regulated as it is critical to ensure that the cellular identity and function are correctly relayed to daughter cells (McIntosh & Hays, 2016, Palozola, Lerner et al., 2019). The major molecular changes occurring during mitosis include a striking decrease in transcription (Prescott & Bender, 1962), condensation of the chromatin (Antonin & Neumann, 2016), nuclear envelope breakdown (Robbins & Gonatas, 1964), and loss of long-range intra-chromosomal interactions (Naumova et al. 2013; Dileep et al. 2015; Stevens et al. 2017).

We have recently conducted a comprehensive study to assess the changes in histone modifications during mitosis (Javasky, Shamir et al., 2018). Our observations, together with other studies (Ginno, Burger et al., 2018, Hsiung, Morrissey et al., 2015, Kelly, Miranda et al., 2010, Kruhlak, Hendzel et al., 2001, Liang, Woodfin et al., 2015, McManus & Hendzel, 2006, Van Hooser, Goodrich et al., 1998) support the following notions: (***i***) the global epigenetic landscape is preserved during mitosis; (***ii***) the mitosis phase encompasses global reduction in histone acetylation; and (***iii***) there is a dramatic increase in histone phosphorylation.

What causes histone deacetylation during mitosis? Histone acetylation is carried out by HATs (Lee & Workman, 2007) and is removed by HDACs (Haberland, Montgomery et al., 2009). HDACs encompass a diverse set of deacetylases that are involved in the regulation of the acetylation levels of histones as well as many other proteins. There are 18 HDACs in mammals that are classified into four major classes based on their homology to yeast HDACs. This categorization includes HDAC1-3 and 8 in Class I, HDAC4-10 in Class II, the sirtuins SIRT1-7 in Class III and HDAC11 in Class IV (Seto & Yoshida, 2014). While some evidence has linked specific HDACs to mitosis, the exact HDAC that conducts the mitotic deacetylations is not well characterized. HDAC3 was suggested to play a key role in human mitosis, since knocking it down in human HeLa cells affects mitosis histone deacetylation (Li, Kao et al., 2006). In yeast, the Hst2p histone deacetylase (SIR2 homologue), was shown to be responsible for the deacetylation of H4K16 during mitosis (Wilkins, Rall et al., 2014). In addition, the mitosis-specific deacetylation of histones could be carried out

by a change in the balance between HATs and HDACs. Evidence supporting this notion was provided by a mass spectrometry-based study that determined the changes in DNA associated proteins between various cell cycle stages and demonstrated a general retention of HDACs and depletion of HATs in mitosis (Ginno et al., 2018).

Here, by using small molecule inhibitors for different HDACs followed by H3K9 deacetylation detection by immunofluorescence, immunoblots and ChIP-seq, we demonstrate that HDAC2, HDAC3 and SIRT1 are all involved in H3K9 deacetylation. Further dissection revealed that HDAC2 deacetylates H3K9 already at prophase whereas HDAC3 is effective only at metaphase. In spite of the extensive overlap between their targets we found a certain degree of specificity. H3K9 in promoters of genes associated with mitosis is preferentially deacetylated by HDAC3. SIRT1 is absent from the mitotic chromatin, however, it affects H3K9 acetylation indirectly through the modulation of mitotic HAT activity. Taken together, our results provide insight into the biochemical pathways involved in histone deacetylation during mitosis and pave the way for further studies aimed to decipher the role of the deacetylation process.

Results

Identification of the deacetylases involved in modulating H3K9ac during mitosis

To study the changes in histone acetylation during mitosis, we focused on H3K9ac, which is reduced approximately by 2.7-fold during mitosis in HeLa-S3 cells (Javasky et al., 2018). To better identify the mitotic stage in which deacetylation takes place, we enriched HeLa-S3 cells for mitotic cells by releasing the cells from a double thymidine block for 8.5 hours. This resulted in primarily G2/M cells with approximately 35% of the cells in mitosis, most of them in the metaphase stage (**Fig. 1a and Appendix Figure S1**). Immunofluorescence of H3K9ac at different mitotic stages revealed that this mark declines at prophase, reaches a minimal level at metaphase, remains low at anaphase and gradually increases at later stages of mitosis (**Fig. 1b**).

To identify the HDACs involved in the decrease in H3K9ac levels in metaphase, we arrested the cells at a metaphase-like stage with monoastral spindles using the kinesin 5 inhibitor STC (Skoufias, DeBonis et al., 2006). We added various HDAC inhibitors for 9 hours (**Fig. 1c**) and measured H3K9ac levels by immunofluorescence (**Fig. 1d**).

We found that treatment with either the pan-HDAC inhibitor, trichostatin A (TSA) (Khan, Jeffers et al., 2008, Lobera, Madauss et al., 2013) or the pan-sirtuin inhibitor, nicotinamide (NAM) (Hu, Jing et al., 2014) induces a significant increase ($P<10^{-23}$; one sided t test) in H3K9ac levels.

We further studied the deacetylation process by using specific inhibitors for particular histone deacetylases. Building on the results of previous studies linking HDAC3 and SIRT1 to mitosis (Fatoba & Okorokov, 2011, Li et al., 2006), we decided to first investigate the involvement of these histone deacetylases. We observed that the HDAC3-specific inhibitor, RGFP966 (Malvaez, McQuown et al., 2013) and the SIRT1-specific inhibitor EX-527 (Hu et al., 2014) induce an increase in mitotic H3K9ac that is similar to the acetylation levels following inhibition with pan-HDAC or pan-sirtuin inhibitors (**Fig. 1d**). Similar results were obtained by immunoblots (**Fig. 1e**).

The deacetylation of H3K9 initiated at prophase (**Fig. 1b**); consequently, it cannot be fully studied by STC synchronization that arrests cells at a metaphase-like stage. Thus, we targeted double-thymidine synchronized cells with the small-molecule inhibitors. The various inhibitors were used upon release from the second thymidine block, and the level of H3K9ac was assessed 8.5 hours later, a time-point that is maximally enriched for cells from all mitotic stages and cytokinesis (**Fig. 1a and Appendix Figure S1**). Cells were binned according to the different mitosis stages (prophase, metaphase, anaphase, and telophase) and cytokinesis, and H3K9ac immunofluorescence intensity was measured separately for each stage (**Fig. 2a**). We found that the general HDAC inhibitor TSA (Khan et al., 2008, Lobera et al., 2013) affects H3K9ac at prophase, while the pan-sirtuin inhibitor NAM (Hu et al., 2014) induces an increase in acetylation levels only in metaphase.

To identify the specific enzyme or enzymes that are involved in mitotic deacetylation, we used small molecules that selectively target a single or a concrete subset of histone deacetylases. In particular, we observed that treatment with RGFP966, an HDAC3-specific inhibitor (Malvaez et al., 2013), affects H3K9ac levels only in metaphase, while treatment with Chidamide that selectively inhibits HDAC1, HDAC2, HDAC3 and HDAC10 (Ning, Li et al., 2012), shows very similar results to TSA. These results suggest that the deacetylation we observed at prophase is probably carried out by

either HDAC1, HDAC2 or HDAC10, given the differential impact of inhibiting HDAC3 alone by RGFP966.

To determine which of the three HDACs (HDAC1, HDAC2 or HDAC10) is modulating H3K9ac during prophase, we used two specific inhibitors – MS-275 that specifically targets HDAC1, HDAC2 and HDAC3 (Khan et al., 2008, Tatamiya, Saito et al., 2004) and CAY10683, an HDAC2 inhibitor (Jaju Bhattad, Jeyarajah et al., 2020, Pavlik, Wong et al., 2013). Following the specific inhibition, we measured H3K9ac levels in cells captured at different stages of mitosis (**Fig. 2a**). We observed that both MS-275 and CAY10683 induced an increase in H3K9 acetylation levels in prophase. However, only MS-275 induced an increase in H3K9 acetylation levels in metaphase as well. This specific pattern suggests that HDAC2 (targeted by CAY10683 and MS-275) deacetylates H3K9ac during prophase, while HDAC3 (targeted by RGFP966 and MS-275) maintains the low acetylation levels from metaphase through telophase.

As mentioned above, the pan-sirtuin inhibitor, nicotinamide (NAM) induces a significant increase in H3K9ac levels as well. To study the involvement of the NAM-target sirtuins in H3K9 deacetylation in mitosis, we used the SIRT1 specific inhibitor, EX-527 (Hu et al., 2014). The effect of SIRT1 inhibition was very similar to that of pan-sirtuin inhibition, suggesting that among the sirtuins, SIRT1 is the main mitotic H3K9 deacetylase.

Finally, we evaluated whether the results we obtained in HeLa-S3 can be reproduced in another system by repeating the main experiments in mouse embryonic fibroblasts (MEFs). To this end, we synchronized the MEFs with a double thymidine block and measured H3K9ac levels by immunofluorescence 8.5 hours after release from the second block. We focused on prophase and metaphase in the MEFs and observed high similarity to the results obtained in the human cell line (HeLa-S3). Specifically, treatment of MEFs with either TSA, Chidamide or MS-257 induced an increase in H3K9ac levels in both prophase and metaphase (**Fig. 2b**). On the other hand, the increased H3K9ac level in MEFS was seen only in metaphase when treated with NAM, EX-527, or RGFP966, and only in prophase when treated with CAY10683 (**Fig. 2b**).

Taken together, our results suggest that mitosis-associated H3K9 deacetylation is a two-stage process – HDAC2 performs deacetylation during prophase, and HDAC3 and SIRT1 subsequently maintain low acetylation levels in metaphase.

Variations in the mitotic chromosome localization of key histone deacetylases and histone acetyltransferases.

Our finding that the deacetylation process is dependent on HDAC2, HDAC3 and SIRT1, suggests that these deacetylases are associated with the mitotic chromosomes. We carried out immunofluorescence experiments targeting key HDACs and sirtuins to evaluate their mitotic localization. Using our double thymidine synchronization scheme (**Fig. 1a**), we observed that among the HDACs tested, only HDAC3 was retained on the mitotic chromosomes during all of the mitotic stages. On the other hand, HDAC1 and HDAC2 appeared to be associated with the mitotic chromosomes at lower levels only during prophase (**Fig. 3a**). Surprisingly, even though we observed that inhibition of SIRT1 brings about an increase in H3K9ac during metaphase, neither SIRT1 nor the other sirtuins we tested (SIRT2, SIRT6 and SIRT7) showed strong binding to the chromatin in metaphase. While we observed low binding of SIRT1 during prophase, there was a reduction in its localization from metaphase for the duration of mitosis (**Fig. 3b**).

We performed similar experiments with several histone acetyl transferases and, observed that HAT1 and EP300, but not CBP and GCNL2, retained their binding to the mitotic chromosomes (**Fig. 3c**). Next, we validated these results by a immunoblotting of chromatin from metaphase (STC arrested) and interphase cells. In a similar manner to the immunofluorescence experiments, we detected a signal only for HDAC3, HAT1 and EP300 from the metaphase chromatin fraction. On the other hand, using mitotic chromatin we could not identify a signal for HDAC1, HDAC2, SIRT1, 2, 6 and 7 or two of the HATs – CBP and GCNL2 (**Fig. 3d**). Together, the localization of HDAC2 to mitotic chromatin at prophase and the binding of HDAC3 throughout mitosis, are in line with the two-stage model presented above, while the binding of SIRT1 at prophase was unexpected.

SIRT1 indirectly impacts H3K9ac levels potentially by modulating HAT activity

We considered two hypotheses to reconcile our seemingly contradictory observations, namely, that SIRT1 inhibition impacts H3K9ac levels during mitosis whilst also

showing low binding to chromatin during mitosis. One option is that SIRT1 directly deacetylates H3K9 prior to metaphase, before it detaches from the mitotic chromosomes. However, we ruled out this possibility since inhibition of SIRT1 by EX-527 does not appear to impact the prophase levels of H3K9ac (**Fig. 2a**). The second option we considered is that SIRT1 indirectly impacts metaphase H3K9ac levels by modulating the activity of other histone deacetylases or acetyl transferases.

First, we developed in vitro assays to study SIRT1's impact on histone acetyl transferase activity in metaphase (**Fig. 4**). We isolated protein extracts from STC-arrested HeLa-S3 cells either treated or untreated with the SIRT1 inhibitor EX-525. The extracts were used to acetylate His-tagged histone H3 peptide, and HAT activity was studied by two methods. We used a colorimetric assay that measures the amount of Co-A released in the acetylation reaction via the DTNB absorbance at 412nm (Foyn, Thompson et al., 2017). We also immunoprecipitated the His-tagged histone H3 peptide using nickel beads and evaluated its acetylation level by immunoblot using an H3K9ac antibody. Both assays revealed that HAT activity was increased in extracts made from cells treated with the SIRT1 inhibitor Ex-527 (**Fig. 4a-b**), suggesting that SIRT1 represses the cellular HAT activity during the metaphase stage.

Secondly, we decided to focus on HDAC3 activity, as we observed that HDAC3 is the only histone deacetylase that is localized to the chromatin at metaphase (**Fig. 3**) and appears to be the main histone deacetylase involved in regulating metaphase H3K9ac (**Fig. 2a**). To evaluate the impact of SIRT1 on HDAC3 activity at metaphase, we immunoprecipitated HDAC3 from STC-arrested mitotic cells treated or untreated with EX-527. We then used acetylated His-tagged histone H3 peptide and measured H3K9ac levels by immunoblot. We observed that inhibition of SIRT1 does not impact the deacetylase activity of HDAC3 towards H3K9ac (**Fig. 4c**). Taken together, we show that SIRT1 appears to indirectly affect H3K9ac levels by modulating the mitotic HAT activity. This result is in line with the observation that SIRT1 is mostly detached from the chromosomes during mitosis (**Fig. 3b**).

HDAC2 and HDAC3 activity regulate both common and unique genomic loci.

The results described above, suggest that deacetylation of H3K9 is performed by HDAC2 in prophase and by HDAC3 in metaphase, with SIRT1 indirectly causing additional metaphase H3K9ac reduction via modulation of HAT activity. However,

these results were obtained by immunofluorescence and immunoblots, and thus do not provide information about the modulation of histone acetylation at a genomic level by these deacetylases.

To further study the specific involvement of each of these histone deacetylases in modulating H3K9 during metaphase, we performed ChIP-seq for H3K9ac on STC-arrested cells, either treated or untreated with CAY10683 (HDAC2 inhibitor), RGFP966 (HDAC3 inhibitor), MS-275 (HDAC2 and HDAC3 inhibitor) and EX-527 (SIRT1 inhibitor). To quantitatively compare between the ChIP-seq experiments we used the ChIP-Rx approach (Orlando, Chen et al., 2014) which normalizes the efficiency of ChIP by the addition of identical chromatin from a distinct organism to every reaction. To this end, we added chicken chromatin (harvested from 50,000 untreated and unsynchronized DT-40 cells) to each ChIP-seq reaction. As expected, the chicken chromatin presented a strong enrichment of H3K9ac at promoters, enhancers and insulators, thus validating our ChIP-seq conditions. We used the chicken promoter occupancy to normalize for the differences in ChIP efficiency between the samples (**Fig. 5a and Appendix Figure S2)**.

H3K9ac is expected to be enriched in promoters, enhancers and insulators as we observed previously (Javasky et al., 2018, Zhou, Goren et al., 2011). Indeed, we observed such peaks in our ChIP-seq data for all conditions (**Fig. 5b**). We normalized the different ChIP-seq according to the efficiency of the ChIP-seq in the chicken (**Methods**) and compared H3K9ac occupancy at promoters, enhancers and insulators in the different conditions (**Fig. 5c**). In line with previous results by us and others (Javasky et al., 2018, Palozola et al., 2019), H3K9ac levels were high in unsynchronized (interphase) cells, whereas the acetylation declines during mitosis in untreated cells. However, treatment by the different inhibitors resulted in distinct changes to the ChIP-seq signal. In particular, the HDAC2 inhibitors (CAY10683 and MS-275) and the SIRT1 inhibitor (EX-527) induce a similar increase in the H3K9ac levels at promoters, enhancers and insulators.

On the other hand, treatment with the HDAC3 inhibitor (RGFP966) had very limited impact on the levels of H3K9ac at promoters, enhancers and insulators (**Fig. 5c**), even though the general signal to noise ratio of the ChIP-seq, evaluated by the comparing the data obtained from spiked in chicken chromatin, was similar between all

conditions (**Fig. 5a and Appendix Figure S2**). Further, we anticipated that the ChIP-seq of the cells treated by RGFP966 will show a gain in H3K9ac signal that corresponds to the global increase in the level of this mark we observed by immunofluorescence and immunoblot experiments (**Fig. 1** and **Fig. 2**). We hypothesize that the regions that are highly impacted by inhibition of HDAC3 could potentially be located in genomic loci that are not amenable to ChIP-seq analysis, such as centromeric regions. We further consider the potential options for this discrepancy in Discussion.

To better understand the differences in the mitotic deacetylation activities of HDAC2 and HDAC3 we used EdgeR to identify the differentially-occupied peaks in cells treated with RGFP966 and CAY10683. We found that the vast majority of the peaks were affected similarly by the two inhibitors and only approximately 8% of the peaks were differentially occupied (**Fig. 5d and Appendix Figure S4**). GO annotation analysis revealed that the RGFP966-specific regions are significantly enriched for genes involved in mitotic regulation and in mRNA metabolism (**Fig. 5e and Appendix Figure S5**).

Discussion

Multiple studies have demonstrated that there is a process of histone deacetylation during mitosis (Palozola et al., 2019). However, the mechanism underlying this process has not previously been studied in depth. Here, we combined molecular and genomic techniques to measure the impact of inhibiting specific histone deacetylases, and were able to identify the key regulators involved in the mitosis-associated deacetylation of H3K9ac – HDAC2, HDAC3 and SIRT1 (**Fig. 2**). We found that HDAC2 deacetylates H3K9 in prophase and HDAC3 deacetylates during metaphase. In spite of the extensive overlap between their targets there is a certain degree of specification in which HDAC3 preferably deacetylates promotors of genes associated with mitosis. While we observed that SIRT1 becomes detached from the chromatin during mitosis, we show that this sirtuin affects H3K9ac via repression of mitotic HAT activity.

While inhibition of HDAC2 increases H3K9ac levels at prophase, the acetylation decreases again in metaphase, most probably due to HDAC3 activity. Indeed, when we inhibited both HDAC2 and HDAC3 we observed an increase in H3K9ac levels

throughout mitosis. On the other hand, HDAC3 inhibition did not affect H3K9ac levels at prophase (probably due to the activity of HDAC2) but showed increased H3K9ac levels at metaphase. These results suggest that HDAC3 has distinct genomic targets that are acetylated only when HDAC3 activity is inhibited. By performing ChIP-seq on STC-arrested cells treated with the various HDACs inhibitors we identified the spatial activity of each of the HDACs. We found that HDAC2 inhibition has a much larger effect on promoters, enhancers and insulators, than HDAC3 inhibition (**Fig. 5c**). Yet, there are certain genomic regions that are preferably deacetylated by HDAC3 (**Fig. 5d and Appendix Figure S4**), including the promoters of genes important for mitotic entry, suggesting that the deacetylation of these genes is done specifically by HDAC3 at metaphase and not beforehand by HDAC2 in prophase. Delaying the deacetylation of those mitotic genes may serve as a means for delaying their transcription shut down allowing a lingered expression during mitosis.

The increased levels of H3K9ac upon HDAC3 inhibition can only be partially explained by the genomic regions uniquely affected by it. In addition, we cannot rule out other effects of HDAC3 that cannot be observed by ChIP-seq. For example, it has been shown that HDAC3 plays a role in deacetylation of centromere histones (Eot-Houllier, Fulcrand et al., 2008). In addition, in yeast, besides the association of H3K9ac with transcription, it was shown that there are genome-wide low levels of H3K9ac, which are associated with DNA replication (Bar-Ziv, Voichek et al., 2016). If such a mechanism also exists in mammals, an appealing hypothesis is that HDAC3 is responsible for erasing this replication-associated acetylation. Indeed, HDAC3 was shown to be associated with DNA replication in mammalian cells (Kylie, Romero et al., 2016) and HDAC3 null mouse cells show replication defects and DNA damage (Bhaskara, Chyla et al., 2008). Further analysis of HDAC2 and HDAC3 localization during mitosis is needed to support this hypothesis.

The resumption of H3K9ac starts, under normal growth conditions, at anaphase (**Fig. 1b**). We found that two HATs (HAT1 and EP300) remain associated with the mitotic chromosomes at all mitosis stages (**Fig. 3**), however, HAT activity during metaphase is reduced indirectly by SIRT1 (**Fig. 4a-b**). This suggests that H3K9ac is delayed to anaphase due to the modulation of HAT activity by post translation modification (PTM). Indeed, SIRT1 inhibition causes an increase in H3K9ac levels already at metaphase (**Fig. 2**). Modulation of HAT activity by PTMs is a well-documented

phenomenon. Many of the HATs are activated by PTMs (Pavlik et al., 2013) and particularly they are frequently activated by auto-acetylation (McCullough & Marmorstein, 2016). Thus, it is reasonable to assume that HAT deacetylation may serve as a tool to repress them. Indeed, it was shown the EP300 is repressed by SIRT1-mediated deacetylation at Lysine residues 1020/1024 (Bouras, Fu et al., 2005). Our observation is in line with these observations and suggests a physiological role for the regulation of HATs by SIRT1 at mitosis.

Our results suggest that the low levels of H3K9ac during mitosis is achieved by a combination of two HDACs and by the modulation of HAT activity by a third HDAC. Indeed, it was shown previously that the sole inhibition of class I and II HDACs by sodium butyrate is not sufficient to achieve full acetylation during mitosis due to the decreased ability of HATs to act on histones in mitotic chromatin (Patzlaff, Terrenoire et al., 2010). It has been shown that RNA polymerase and many of the transcription factors fall off the mitotic chromatin (Kadauke & Blobel, 2013, Martinez-Balbas, Dey et al., 1995, Parsons & Spencer, 1997). Yet, the assumption that almost all transcription regulators are displaced from the chromatin during mitosis was recently challenged by a mass-spectrometry based study that showed a large-scale retention of TFs and preinitiation complex members on the mitotic chromatin (Ginno et al., 2018). Indeed, our results regarding the mitotic localization of several histone acetylases and deacetylases support the more complex picture of partial retention of transcription regulators on the mitotic chromatin (**Fig. 3**). We found that HDAC1 and HDAC2 fall off the chromatin only at metaphase whereas HDAC3 remains on the chromatin in all mitosis stages. The sirtuins show a partial chromatin association at prophase and they are not seen at the chromatin from metaphase on. Finally, we found that some of the HATs (EP300 and HAT1) remain on the chromatin while others (CBP and GCN5L2) fall off. These results are only partially consistent with previous observations. The displacement of HDAC1 and HDAC2 from metaphase to the end of mitosis was reported previously in MCF7 cells (He, Khan et al., 2013). On the other hand, HDAC3 was found on mitotic chromatin in HeLa-S3 cells (Li et al., 2006) but not on MEFs (Bhaskara et al., 2008). Similarly, SIRT1 was found by us to evict the mitotic chromosomes at the metaphase stage in HeLa-S3 cells (**Fig. 3**), while in MEFs it seems to be retained on the chromatin along all mitotic stages (Fatoba & Okorokov, 2011). These discrepancies are either due to the use of different techniques or due to

the use of different experimental systems. Further research is needed in order to determine whether the different results reflect differences between primary and transformed cells.

Our conclusions are based on the use of small-molecule HDACs inhibitors, which are known to be specific for various HDACs (**Table 1**). To avoid high-dependency on the specificity of each of the small molecules, we aimed to employ multiple inhibitors to target key deacetylases. Thus, we evaluated the involvement of HDAC2 by using MS-275, Chidamide and CAY10683 and studied HDAC3 by using RGFP966, Chidamide and MS-275 (**Table 1**). However, for SIRT1 we could only use EX-527, and thus, we currently cannot rule out the involvement of additional sirtuins in the process and further research is required to study this possibility.

Taken together, our results suggest a complex mechanism for H3K9 deacetylation during mitosis. It is carried out by a combination of HDACs that are activated at different stages and by delaying HAT activity by SIRT1. Furthermore, it seems that there is spatial separation in the activity of the HDACs with HDAC2 acting already at prophase on most transcription-associated H3K9ac peaks, whereas HDAC3 contributes at a later stage and deacetylates mitosis-specific genes and additional clustered genomic regions not affected by HDAC2. Further research is needed for studying the consequence of each wave of deacetylation on mitotic traits such as transcription repression and chromosome condensation.

Methods

Cell culture and cell cycle synchronization

HeLa-S3 cells and MEFs were grown in Dulbecco's Modified Eagle's Medium (DMEM) supplemented with 10% fetal bovine serum (FBS), penicillin-streptomycin, L-glutamine, sodium pyruvate, and 0.1% Pluronic F-68. Cells were incubated at 37°C and 5% CO_2. DT40 cells were cultured in RPMI 1640 medium supplemented with 10% fetal calf serum, 1% chicken serum, 10 mM HEPES and 1% penicillin-streptomycin mixture at 39.5 °C with 5% CO_2.

For STC mitotic arrest, cells were pre-synchronized in G1/S by addition of 2 mM thymidine for 16 h, washed with PBS, released for 3 h in fresh medium, and arrested

with 10μM S-trityl-L-cysteine (STC) (164739, Sigma) for 12 h. For double thymidine synchronization**,** HeLa-S3 cells were grown on coverslips in Dulbecco's Modified Eagle's Medium (DMEM) supplemented with 10% foetal bovine serum (FBS), penicillin-streptomycin, L-glutamine, sodium pyruvate, and 0.1% Pluronic F-68. Cells were incubated at 37°C and 5% CO^2. Cells were grown for 20 h, treated with 2 mM thymidine for 18 h, washed with PBS, released for 8 h in fresh medium, treated with 2 mM thymidine for 17 h, washed with PBS, released for 8.5 h in fresh medium, and harvested.

HDAC and sirtuin inhibitors

The concentrations and specificities of the inhibitors we used are summarized in **Table 1.** The inhibitors were added for 8.5-9 hours (**Fig. 1a and C**).

Chromatin isolation

Chromatin was isolated from STC-synchronized HeLa-S3 cell line using a previously published protocol (Sone, Iwano et al., 2002). Synchronized cells were collected by centrifugation and resuspended into a hypotonic solution of 75mM KCL (pH 5.7). After treatment of KCL hypotonic solution for 30 min, the cells were collected by centrifugation and resuspended into CAS buffer (0.1 M citric acid, 0.1 M sucrose, 0.5% Tween 20, pH 2.6). After lysis of the cell membrane in CAS buffer, the chromatin suspension was centrifuged at 190g for 3 min at 4°C. The chromatin-rich fraction was carefully recovered as supernatant and the nuclei rich fraction was recovered as the precipitation. The supernatant fraction was then centrifuged again at 1750g for 10 min at 4°C. The precipitated chromatin was resuspended in CAS buffer containing 0.1 mM phenylmethylsulfonyl fluoride. The isolated mitotic chromatin quantity was estimated by BCA method and stored in -80°C until further use.

Chromatin from asynchronous cells was isolated as described (Torrente, Zee et al., 2011). Cells were resuspended in Buffer A (10 mM HEPES pH=7.9, 10 mM KCl, 1.5 mM MgCl2, 0.34 M sucrose, 10% glycerol, inhibitor cocktail: 1 mM DTT, 0.5 mM 4-(2-aminoethyl) benzenesulfonyl fluoride hydrochloride and protease inhibitor cocktail). Triton X-100 was added to a final concentration of 0.1% and the suspension was incubated for 8 minutes on ice. The nuclear pellet was obtained by centrifugation (1,300g for 5 minutes at 4°C), washed with Buffer A and then resuspended in Buffer

B (3 mM EDTA, 0.2 mM EGTA, and protease inhibitor cocktail) for 30 minutes on ice. The insoluble chromatin pellet was isolated by centrifugation (1,700g for 5 minutes at 4°C) and then resuspended in 15 mM Tris, pH=7.5, 0.5% SDS. The isolated mitotic chromatin quantity was estimated by BCA method and stored in -80°C until further use.

Immunoblot

Isolated chromosomes were directly suspended and dissolved in SDS sample buffer (62.5 mM Tris-HCl (pH 6.8), 5% 2-mercaptoethanol, 20% glycerol, 2% SDS, and 0.005% bromophenol blue). Purified chromatin was separated by SDS-PAGE and transferred to 0.45 μm polyvinylidene difluoride membranes (Immobilon, Millipore, Merck KGaA, Darmstadt, Germany). Blots were incubated with primary antibodies HDAC1 (Cell Signalling # D5C6U; 1;1000), HDAC2 (Cell Signalling #D6S5P; 1:1000), HDAC3 (Cell Signalling #7G6C5; 1;1000), CBP(Cell Signalling #D6C5;1;1000),GCN5L2(Cell Signalling #C26A10; 1:1000),P300(Santacruze #sc-48343; 1:100) HAT-1(Santacruze # sc-390562; 1:1000), SIRT1(Cell Signalling #8469; 1;1000), SIRT2 (Santacruze #sc-28298; 1:1000), SIRT6 (Abcam #ab62739; 1:1000) and SIRT7 (Santacruze #135055; 1:1000), histone H3 acetyl K9 (Ac-H3K9; (Cell Signalling #C5B11; 1:1000). HRP-conjugated secondary antibodies (Jackson Immuno Research #111-035-003 and #115-035-003; 1:5000) were used. Immunoblots were developed with an ECL-plus kit. Equal loading of protein in each lane was verified by histone H3 (Cell Signalling #D1H2; 1:1000).

Immunofluorescence staining

For immunofluorescence studies, HeLa-S3 cells and MEFs were grown on coverslips, blocked in PBS containing 5% BSA and 0.1% Triton X-100. Cells were then incubated with a primary antibody - HDAC1 (Cell Signalling # D5C6U; 1:100), HDAC2 (Cell Signalling# D6S5P; 1:1000), HDAC3 (Cell Signalling #7G6C5; 1:100), CBP (Cell Signalling #D6C5; 1:100), GCN5L2 (Cell Signalling #C26A10; 1:100), P300 (Santacruze #sc-48343; 1:100), HAT-1 (Santacruze # sc-390562; 1:100), SIRT1 (Cell Signalling #8469; 1;100), SIRT2 (Santacruze #sc-28298; 1:100), SIRT6 (Abcam # ab62739; 1:100) and SIRT7 (Santacruze #135055; 1:100), H3K9ac (Cell Signalling #C5B11; 1:400) overnight at 4°C. After washing, cells were incubated with an anti-rabbit IgG or anti-mouse IgG conjugated to FITC probes (Invitrogen #A11034 and

#A11001) for 1 h at room temperature (RT). After washing, slides were mounted with SlowFade Gold antifade reagent with DAPI (Sigma) and immunofluorescent signals were viewed using an Olympus fluorescence microscope. Images were analysed with ImageJ (Fiji version) to quantify mean intensity/pixel in the DAPI stained regions.

In Vitro HAT Activity Assay

In vitro histone acetylation assays were performed on 25 µg of mitotic chromatin (isolated as described above and quantified using the bicinchoninic acid colorimetric assay system (Sigma)) in 50 mM Tris-HCL, 10% glycerol, 1mM DTT, 1mM PMSF, 50nM TSA, 0.1 mM EDTA supplemented with 100µM Acetyl-CoA and 10 µg His-tagged Histone H3 (BPS Bioscience #52023). The reaction was incubated at 37°c for 1 h. HAT activity was quantified by: i) a colorimetric assay quantifying the release of Co-A using DTNB (2-nitrobenzoic acid) (Sigma) by measuring the absorbance at 412nm; ii) isolating the His-tagged H3 by Ni-NTA column and measuring H3K9ac by immunoblots using anti-H3K9Ac antibody (Cell Signalling # C5B11; 1:1000). All acetylation assays were performed in duplicate.

In vitro HDAC3 Activity Assay

Mitotic HeLa-S3 cells were lysed in cell lysis buffer (0.5% NP-40, 20 mM Tris-HCl (pH 7.4), 500 mM NaCl, 0.5 mM EGTA, 10% Glycerol, 0.5% Triton-X 100, complete protease inhibitor cocktail and 1 µM of zinc citrate.). Mitotic lysate was precleared by the protein A magnetic bead (Cell signalling) for 20 min at room temperature. After protein quantification by the bicinchoninic acid colorimetric assay system (Sigma), 1mg protein samples were used for HDAC3 immunoprecipitation using four microliters of HDAC3 antibodies (Cell Signalling) and incubated at 4 °C overnight, followed by 2 h incubation with 20 µL protein A magnetic beads. The captured beads were rinsed with lysis buffer five times and i) boiled in 5× SDS loading buffer for 5 min for confirming HDAC3 immunoprecipitation by immunoblot (after brief centrifugation, supernatants were loaded onto 12% SDS-PAGE gels and detected using rabbit-anti-HDAC3 antibody (1:1000; cell signalling) and HRP-conjugated secondary antibodies). Or ii) immunocomplex was eluted from bead in 0.2 M glycine pH 2.6 by incubating the sample for 10 minutes and neutralized by adding equal volume of Tris-HCL pH 8.0, and stored at -20°c for further use.

To perform HDAC activity assay, we used 50 ng of immunoprecipitated HDAC3 and 4µg of His-tagged H3 (BPS Bioscience #52023; acetylated by pre-treatment with whole cell extract and isolated by Ni-NTA column), in HDAC Assay buffer (10 mM Tris-HCl (pH 8.0), 10 mM NaCl, 1 µM ZnSO4 10% glycerol, and complete protease inhibitor mixture), incubated at 37°C for 1hrs. After the incubation, SDS-PAGE loading buffer is added to the reaction and runs on 12% SDS-PAGE. HDAC3 activity in the presence or absence of inhibitors was assessed by immunoblotting using anti H3K9ac antibody (Cell Signalling # C5B11; 1:1000).

ChIP-seq

ChIP experiments were carried out as described in (Mikkelsen, Ku et al., 2007). All ChIP experiments were carried out on $2X10^5$ cells. $1.5X10^5$ HeLa-S3 cells (unsynchronized or STC synchronized with or without the indicated treatments) and $0.5X10^5$ unsynchronized and untreated DT-40 cells were cross-linked with 4% formaldehyde and mixed. The cell mixture was lysed and sonicated by Covaris to obtain an average chromatin size of 200-700 bp. Immunoprecipitation, using anti-H3K9ac (C5B11, Cell Signalling Technology), was carried out with inverting at 4°C for 14–16 h. Antibody-chromatin complexes were pulled-down using Protein A/G magnetic beads (Dy-10001D and Dy-10003D, Invitrogen), washed and then eluted. After cross-link reversal and Proteinase K treatment, immunoprecipitated DNA was extracted with 1.8x Agencourt AMPure XP beads (BCA63881, Beckman Coulter).

Library preparation and sequencing

ChIP DNA (or unenriched whole cell extract) were prepared for Illumina sequencing as described (Yehuda, Blumenfeld et al., 2018). Briefly, DNA was subjected to a 50 µl end repair reaction, cleaned by 1.8× AMPure XP beads, followed by a 50µl A-tail reaction. The products were cleaned and ligated to 0.75 µM Illumina compatible forked indexed adapters. Ligation products were size selected in order to remove free adaptors. Ligation products were amplified with 15 (Input DNA) or 18 PCR cycles (ChIP DNA). Amplified DNA was size selected for 300–700 bp fragments using AMPure XP beads. The final quality of the library was assessed by Qubit and TapeStation. Libraries were pooled and sequenced on NextSeq (Illumina), using a

paired-end protocol. The sequencing depth of each library is provided at Appendix Table S1.

Bioinformatic analysis

ChIP-seq reads were aligned to the human genome (hg38) using Bowtie2 (Langmead & Salzberg, 2012). All regions listed in the ENCODE hg38 blacklist, were excluded from all analyses. Duplicate alignments were removed with Picard Tools MarkDuplicates (http://broadinstitute.github.io/picard/). Only reads with mapping quality > 30 were used in the analysis. Peak detection on merged unsynchronized replicates (with a whole cell extract dataset as a control) was done using MACS2 (Zhang, Liu et al., 2008) with default parameters and q-value of 0.05.

Metagene analyses were done using the python package Metaseq (Dale, Matzat et al., 2014). The metagenes were aligned to human transcription start sites (n=60580, taken form ENSEMBL GTF files), enhancers and insulators (n=4274 and 2025, respectively, taken from (Javasky et al., 2018)); and to chicken TSS (n=7234, taken form ENSEMBL GTF files), enhancers (n= 20633, retrieved from the enhancer atlas (Gao & Qian, 2020), and insulators (n=13510 CTCF binding sites, retrieved from GSM1253767). All datasets were normalized according to the Chicken promoter data.

IGV snapshots show TDF files created from the aligned sequence data (using the count command from IGV tools (Robinson, Thorvaldsdottir et al., 2011, Thorvaldsdottir, Robinson et al., 2013). The scale of each track was adjusted to the total number of reads multiplied by a normalization factor derived from the chicken promoter data.

PCA was done using the R function prcomp with the data shifted to be zero centered.

RGFP966 and CAY10683 specific peaks were identified using EdgeR using all replicates of each condition and the list of all peaks from the unsynchronized data. Significant peaks were determined with FDR < 0.05.

GO annotation analysis was performed using the Toppgene tool (Chen, Bardes et al., 2009) using only peaks that were adjacent to TSS (+/- 2Kb). The entire set of H3K9ac

peaks (adjacent to TSS) were used as background. Biological process GO annotation with an FDR corrected p-val<0.05 are shown.

Data availability

The Chip-Seq datasets produced in this study are available in Gene Expression Omnibus GSE168180. (reviewer token – **uzwteuquldevrix)**

Figure legends

Fig1. H3K9ac levels during mitosis (A) Schematic representation of the synchronization strategy by double thymidine block method. **(B)** Immunofluorescence of HeLa-S3 cells enriched for mitotic stages stained for H3K9ac (green), and DNA (blue). Representative pictures from the major mitosis stages are shown. Quantification of the immunofluorescence results presented below the pictures. Intensity values represent the mean ± SEM of at least 20 cells for every stage. **(C)** Schematic representation of the synchronization strategy by kinesin-5 inhibitor S-trityl-L-cysteine (STC). **(D)** Immunofluorescence of STC arrested HeLa-S3 cells stained for DNA (blue) and H3K9ac (green). The cells were either not treated (N.T.) or treated with TSA (150nM); Nicotinamide (NAM, 10mM); RGFP966 (40µM); EX-527 (5nM). Quantification of the immunofluorescence results are shown below the pictures. Intensity values represent the mean ± SEM of at least 25 cells for every condition. All treatments significantly ($P<10^{-23}$; one sided ttest) increased H3K9ac levels **(E)** Immunoblot showing the H3K9ac signal for synchronized HeLa-S3 cells treated with the indicated inhibitors (same concentration as in D), total histone H3 serves as a loading control.

Fig2. Effects of HDAC inhibitors of H3K9ac dynamics during mitosis (A) Immunofluorescence of HeLa-S3 cells enriched for mitotic stages stained for H3K9ac (green), and DNA (blue). Representative pictures from the major mitosis stages are shown. The cells were either not treated (N.T.) or treated with TSA (150nM); Nicotinamide (NAM, 10mM); RGFP966 (40µM); Chidamide (10µM); EX-527 (5nM); CAY10683 (1µM); MS-275 (1µM). Below, quantification of the immunofluorescence results. Intensity values represent the mean ± SEM of at least 20 cells for every stage. **(B)** Immunofluorescence of MEFs cells enriched for mitotic

stages stained for H3K9ac (green), and DNA (blue). Representative pictures from the Interphase, Prophase and Metaphase stages are shown. The cells were either not treated (N.T.) or treated with TSA (150nM); Nicotinamide (NAM, 10mM); RGFP966 (40µM); Chidamide (10µM); EX-527 (5nM); CAY10683 (1µM); MS-275 (1µM). Below, quantification of the immunofluorescence results. Intensity values represent the mean ± SEM of at least 20 cells for every stage.

Fig3. Localization of selected chromatin regulators during mitosis Immunofluorescence of HeLa-S3 cells enriched for mitotic stages, stained for DNA (blue) and for various HDACs **(A)**, sirtuins **(B)** and HATs **(C)** (green). Representative pictures from the major mitosis stages and interphase are shown, along with a quantification of at least 20 cells from each stage. Intensity values represent the mean ± SEM. Note that only HDAC3, P300 and HAT-1 are retained on the mitotic chromatin along all mitotic stages, whereas the other proteins show partial retention at prophase. **(D)** Immunoblots showing the abundance of the indicated chromatin modifiers in the chromatin fraction of interphase (L1) and mitotic (L2) HeLa-S3 cells. Total histone H3 serves as loading control.

Fig4. SIRT1 indirectly regulates H3K9ac activity by modulating HAT activity.

(**A**) HAT activity colorimetric assay results (mean +/- standard error, N=2) for HeLa-S3 cells either not treated (N.T.) or treated with EX-527 (5nM). **(B)** Immunoblot analysis showing H3K9 acetylation on His-tagged H3 after HAT activity of HeLa mitotic chromatin either not treated (N.T.) or treated with EX-527 (5nM) on His-tagged H3. Total histone H3 serves as loading control. **(C)** Immunoprecipitation of HDAC-3 tested by Immunoblotting. HDAC-3 antibodies and protein A magnetic beads were used to immunoprecipitate (IP) HDAC3 complexes from 1mg of HeLa mitotic extract either not treated (N.T.) or treated with RGFP966 (40µM) or EX-527 (5nM). (i) Showing ponceau S staining of HDAC3 immunocomplex; (ii) showing Immunoblot using HDAC3 antibodies developed by ECL method; (iii) showing ponceau S staining of HDAC3 activity assay reaction subjected to Immunoblot and (iv) showing Immunoblot analysis of immunoprecipitated HDAC3 activity on acetylated his-tagged H3 protein.

Fig5. HDAC activity at transcriptionally associated regions (A) Metagene plots showing H3K9ac promoter occupancy in chicken DT-40 cells before (left) and after

(right) normalization. (B) IGV representation of approximately 64Kb region (Chr5:43.006M-43.07M) of H3K9ac ChIP-seq results under the indicated conditions. The locations of published promoter, enhancer, and insulator are indicated. (C) Metagenes plots showing H3K9ac occupancy around promoters, enhancers and insulators in HeLa-S3 cells. The data were normalized using the DT-40 promoter data. Similar results were obtained in a biological repeat (**Appendix Figure S3). (D)** Venn diagram showing the common and condition specific H3K9ac peaks. (**E**) GO annotation analysis of the RGFP966 specific peaks. Only main categories are shown, the full list of enriched categories is shown in **Appendix Figure S5**.

Table 1 HDACs inhibitors

NO.	Name	Specificity	Concentration (used)	References:
1	TSA	Pan-HDACs	150 nM	(Khan et al., 2008, Lobera et al., 2013)
2	CHIDAMIDE	HDAC1,2,3,10	10 µM	(Ning et al., 2012)
3	RGFP966	HDAC3	40 µM	(Malvaez et al., 2013)
4	CAY10683	HDAC2 and HDAC6	1 µM	(Jaju Bhattad et al., 2020, Pavlik et al., 2013)
5	MS-275	HDAC-1,2,3	1 µM	(Khan et al., 2008)
6	NICOTINAMIDE	Pan-sirtuins	10 mM	(Hu et al., 2014)
7	EX-527	SIRT-1	5nM	(Hu et al., 2014)

Acknowledgments

We thank the members of the Core Research Facility in the Hebrew University School of Medicine; Dr. Idit Shiff and Dr. Abed Nasereddin for generating genomic data. We thank Avraham Greenberg for critical reading of the manuscript. This work was supported by research grants from the Israel Science Foundation (grant # 184/16 to I.S.), ISF-NSFC (grant #2555/16 to I.S.), The Binational Science Foundation (joint program with NSF; grant # 2019688) and NSF/MCB-BSF (grant # 2003358 to A.G).

Conflict of interest

The authors declare that they have no conflict of interest.

Authors contributions

SG and RM performed all the wet experiments. RM and RR performed the bioinformatics analyses. SG, IS, AG and SE designed the experiments. IS and AG wrote the manuscript.

References

Antonin W, Neumann H (2016) Chromosome condensation and decondensation during mitosis. *Curr Opin Cell Biol* 40: 15-22

Bar-Ziv R, Voichek Y, Barkai N (2016) Chromatin dynamics during DNA replication. *Genome Res* 26: 1245-56

Bhaskara S, Chyla BJ, Amann JM, Knutson SK, Cortez D, Sun ZW, Hiebert SW (2008) Deletion of histone deacetylase 3 reveals critical roles in S phase progression and DNA damage control. *Mol Cell* 30: 61-72

Bouras T, Fu M, Sauve AA, Wang F, Quong AA, Perkins ND, Hay RT, Gu W, Pestell RG (2005) SIRT1 deacetylation and repression of p300 involves lysine residues 1020/1024 within the cell cycle regulatory domain 1. *J Biol Chem* 280: 10264-76

Chen J, Bardes EE, Aronow BJ, Jegga AG (2009) ToppGene Suite for gene list enrichment analysis and candidate gene prioritization. *Nucleic Acids Res* 37: W305-11

Dale RK, Matzat LH, Lei EP (2014) metaseq: a Python package for integrative genome-wide analysis reveals relationships between chromatin insulators and associated nuclear mRNA. *Nucleic Acids Res* 42: 9158-70

Eot-Houllier G, Fulcrand G, Watanabe Y, Magnaghi-Jaulin L, Jaulin C (2008) Histone deacetylase 3 is required for centromeric H3K4 deacetylation and sister chromatid cohesion. *Genes Dev* 22: 2639-44

Fatoba ST, Okorokov AL (2011) Human SIRT1 associates with mitotic chromatin and contributes to chromosomal condensation. *Cell Cycle* 10: 2317-22

Foyn H, Thompson PR, Arnesen T (2017) DTNB-Based Quantification of In Vitro Enzymatic N-Terminal Acetyltransferase Activity. *Methods Mol Biol* 1574: 9-15

Gao T, Qian J (2020) EnhancerAtlas 2.0: an updated resource with enhancer annotation in 586 tissue/cell types across nine species. *Nucleic Acids Res* 48: D58-D64

Ginno PA, Burger L, Seebacher J, Iesmantavicius V, Schubeler D (2018) Cell cycle-resolved chromatin proteomics reveals the extent of mitotic preservation of the genomic regulatory landscape. *Nat Commun* 9: 4048

Haberland M, Montgomery RL, Olson EN (2009) The many roles of histone deacetylases in development and physiology: implications for disease and therapy. *Nat Rev Genet* 10: 32-42

He S, Khan DH, Winter S, Seiser C, Davie JR (2013) Dynamic distribution of HDAC1 and HDAC2 during mitosis: association with F-actin. *J Cell Physiol* 228: 1525-35

Hsiung CC, Morrissey CS, Udugama M, Frank CL, Keller CA, Baek S, Giardine B, Crawford GE, Sung MH, Hardison RC, Blobel GA (2015) Genome accessibility is widely preserved and locally modulated during mitosis. *Genome Res* 25: 213-25

Hu J, Jing H, Lin H (2014) Sirtuin inhibitors as anticancer agents. *Future Med Chem* 6: 945-66

Jaju Bhattad G, Jeyarajah MJ, McGill MG, Dumeaux V, Okae H, Arima T, Lajoie P, Berube NG, Renaud SJ (2020) Histone deacetylase 1 and 2 drive differentiation and fusion of progenitor cells in human placental trophoblasts. *Cell Death Dis* 11: 311

Javasky E, Shamir I, Gandhi S, Egri S, Sandler O, Rothbart SB, Kaplan N, Jaffe JD, Goren A, Simon I (2018) Study of mitotic chromatin supports a model of bookmarking by histone modifications and reveals nucleosome deposition patterns. *Genome Res* 28: 1455-1466

Kadauke S, Blobel GA (2013) Mitotic bookmarking by transcription factors. *Epigenetics Chromatin* 6: 6

Kelly TK, Miranda TB, Liang G, Berman BP, Lin JC, Tanay A, Jones PA (2010) H2A.Z maintenance during mitosis reveals nucleosome shifting on mitotically silenced genes. *Mol Cell* 39: 901-11

Khan N, Jeffers M, Kumar S, Hackett C, Boldog F, Khramtsov N, Qian X, Mills E, Berghs SC, Carey N, Finn PW, Collins LS, Tumber A, Ritchie JW, Jensen PB, Lichenstein HS, Sehested M (2008) Determination of the class and isoform selectivity of small-molecule histone deacetylase inhibitors. *Biochem J* 409: 581-9

Kruhlak MJ, Hendzel MJ, Fischle W, Bertos NR, Hameed S, Yang XJ, Verdin E, Bazett-Jones DP (2001) Regulation of global acetylation in mitosis through loss of histone acetyltransferases and deacetylases from chromatin. *J Biol Chem* 276: 38307-19

Kylie K, Romero J, Lindamulage IK, Knockleby J, Lee H (2016) Dynamic regulation of histone H3K9 is linked to the switch between replication and transcription at the Dbf4 origin-promoter locus. *Cell Cycle* 15: 2321-35

Langmead B, Salzberg SL (2012) Fast gapped-read alignment with Bowtie 2. *Nat Methods* 9: 357-9

Lee KK, Workman JL (2007) Histone acetyltransferase complexes: one size doesn't fit all. *Nat Rev Mol Cell Biol* 8: 284-95

Li Y, Kao GD, Garcia BA, Shabanowitz J, Hunt DF, Qin J, Phelan C, Lazar MA (2006) A novel histone deacetylase pathway regulates mitosis by modulating Aurora B kinase activity. *Genes Dev* 20: 2566-79

Liang K, Woodfin AR, Slaughter BD, Unruh JR, Box AC, Rickels RA, Gao X, Haug JS, Jaspersen SL, Shilatifard A (2015) Mitotic Transcriptional Activation: Clearance of Actively Engaged Pol II via Transcriptional Elongation Control in Mitosis. *Mol Cell* 60: 435-45

Lobera M, Madauss KP, Pohlhaus DT, Wright QG, Trocha M, Schmidt DR, Baloglu E, Trump RP, Head MS, Hofmann GA, Murray-Thompson M, Schwartz B, Chakravorty S, Wu Z, Mander PK, Kruidenier L, Reid RA, Burkhart W, Turunen BJ, Rong JX et al. (2013) Selective class IIa histone deacetylase inhibition via a nonchelating zinc-binding group. *Nat Chem Biol* 9: 319-25

Malvaez M, McQuown SC, Rogge GA, Astarabadi M, Jacques V, Carreiro S, Rusche JR, Wood MA (2013) HDAC3-selective inhibitor enhances extinction of cocaine-seeking behavior in a persistent manner. *Proc Natl Acad Sci U S A* 110: 2647-52

Martinez-Balbas MA, Dey A, Rabindran SK, Ozato K, Wu C (1995) Displacement of sequence-specific transcription factors from mitotic chromatin. *Cell* 83: 29-38

McCullough CE, Marmorstein R (2016) Molecular Basis for Histone Acetyltransferase Regulation by Binding Partners, Associated Domains, and Autoacetylation. *ACS Chem Biol* 11: 632-42

McIntosh JR, Hays T (2016) A Brief History of Research on Mitotic Mechanisms. *Biology (Basel)* 5

McManus KJ, Hendzel MJ (2006) The relationship between histone H3 phosphorylation and acetylation throughout the mammalian cell cycle. *Biochem Cell Biol* 84: 640-57

Mikkelsen TS, Ku M, Jaffe DB, Issac B, Lieberman E, Giannoukos G, Alvarez P, Brockman W, Kim TK, Koche RP, Lee W, Mendenhall E, O'Donovan A, Presser A, Russ C, Xie X, Meissner A, Wernig M, Jaenisch R, Nusbaum C et al. (2007) Genome-wide maps of chromatin state in pluripotent and lineage-committed cells. *Nature* 448: 553-60

Ning ZQ, Li ZB, Newman MJ, Shan S, Wang XH, Pan DS, Zhang J, Dong M, Du X, Lu XP (2012) Chidamide (CS055/HBI-8000): a new histone deacetylase inhibitor of the benzamide class with antitumor activity and the ability to enhance immune cell-mediated tumor cell cytotoxicity. *Cancer Chemother Pharmacol* 69: 901-9

Orlando DA, Chen MW, Brown VE, Solanki S, Choi YJ, Olson ER, Fritz CC, Bradner JE, Guenther MG (2014) Quantitative ChIP-Seq normalization reveals global modulation of the epigenome. *Cell Rep* 9: 1163-70

Palozola KC, Lerner J, Zaret KS (2019) A changing paradigm of transcriptional memory propagation through mitosis. *Nat Rev Mol Cell Biol* 20: 55-64

Parsons GG, Spencer CA (1997) Mitotic repression of RNA polymerase II transcription is accompanied by release of transcription elongation complexes. *Mol Cell Biol* 17: 5791-802

Patzlaff JS, Terrenoire E, Turner BM, Earnshaw WC, Paulson JR (2010) Acetylation of core histones in response to HDAC inhibitors is diminished in mitotic HeLa cells. *Exp Cell Res* 316: 2123-35

Pavlik CM, Wong CY, Ononye S, Lopez DD, Engene N, McPhail KL, Gerwick WH, Balunas MJ (2013) Santacruzamate A, a potent and selective histone deacetylase inhibitor from the Panamanian marine cyanobacterium cf. Symploca sp. *J Nat Prod* 76: 2026-33

Prescott DM, Bender MA (1962) Synthesis of RNA and protein during mitosis in mammalian tissue culture cells. *Exp Cell Res* 26: 260-8

Robbins E, Gonatas NK (1964) The Ultrastructure of a Mammalian Cell during the Mitotic Cycle. *J Cell Biol* 21: 429-63

Robinson JT, Thorvaldsdottir H, Winckler W, Guttman M, Lander ES, Getz G, Mesirov JP (2011) Integrative genomics viewer. *Nat Biotechnol* 29: 24-6

Seto E, Yoshida M (2014) Erasers of histone acetylation: the histone deacetylase enzymes. *Cold Spring Harb Perspect Biol* 6: a018713

Skoufias DA, DeBonis S, Saoudi Y, Lebeau L, Crevel I, Cross R, Wade RH, Hackney D, Kozielski F (2006) S-trityl-L-cysteine is a reversible, tight binding inhibitor of the human kinesin Eg5 that specifically blocks mitotic progression. *J Biol Chem* 281: 17559-69

Sone T, Iwano M, Kobayashi S, Ishihara T, Hori N, Takata H, Ushiki T, Uchiyama S, Fukui K (2002) Changes in chromosomal surface structure by different isolation conditions. *Arch Histol Cytol* 65: 445-55

Tatamiya T, Saito A, Sugawara T, Nakanishi O (2004) Isozyme-selective activity of the HDAC inhibitor MS-275. *Cancer Research* 64: 567-567

Thorvaldsdottir H, Robinson JT, Mesirov JP (2013) Integrative Genomics Viewer (IGV): high-performance genomics data visualization and exploration. *Brief Bioinform* 14: 178-92

Torrente MP, Zee BM, Young NL, Baliban RC, LeRoy G, Floudas CA, Hake SB, Garcia BA (2011) Proteomic interrogation of human chromatin. *PLoS One* 6: e24747

Van Hooser A, Goodrich DW, Allis CD, Brinkley BR, Mancini MA (1998) Histone H3 phosphorylation is required for the initiation, but not maintenance, of mammalian chromosome condensation. *J Cell Sci* 111 (Pt 23): 3497-506

Wilkins BJ, Rall NA, Ostwal Y, Kruitwagen T, Hiragami-Hamada K, Winkler M, Barral Y, Fischle W, Neumann H (2014) A cascade of histone modifications induces chromatin condensation in mitosis. *Science* 343: 77-80

Yehuda Y, Blumenfeld B, Mayorek N, Makedonski K, Vardi O, Cohen-Daniel L, Mansour Y, Baror-Sebban S, Masika H, Farago M, Berger M, Carmi S, Buganim Y, Koren A, Simon I (2018) Germline DNA replication timing shapes mammalian genome composition. *Nucleic Acids Res* 46: 8299-8310

Zhang Y, Liu T, Meyer CA, Eeckhoute J, Johnson DS, Bernstein BE, Nusbaum C, Myers RM, Brown M, Li W, Liu XS (2008) Model-based analysis of ChIP-Seq (MACS). *Genome Biol* 9: R137

Zhou VW, Goren A, Bernstein BE (2011) Charting histone modifications and the functional organization of mammalian genomes. *Nat Rev Genet* 12: 7-18

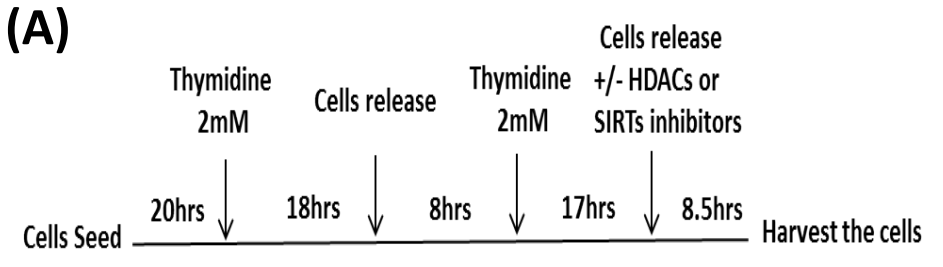
(A)
Thymidine 2mM
Cells release
Thymidine 2mM
Cells release +/- HDACs or SIRTs inhibitors
Cells Seed
20hrs
18hrs
8hrs
17hrs
8.5hrs
Harvest the cells

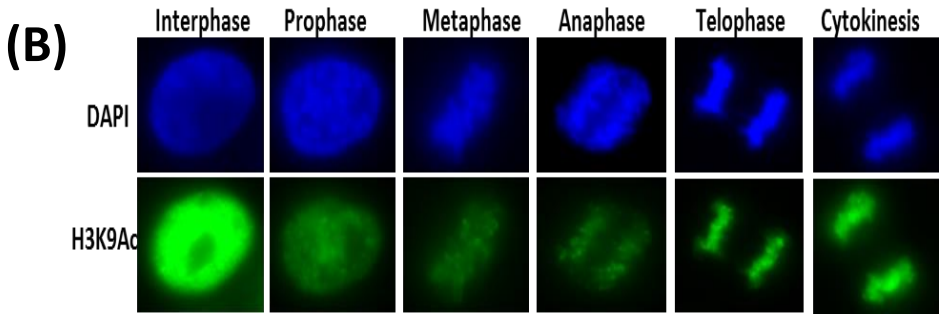
(B)
Interphase
Prophase
Metaphase
Anaphase
Telophase
Cytokinesis
DAPI
H3K9Ac

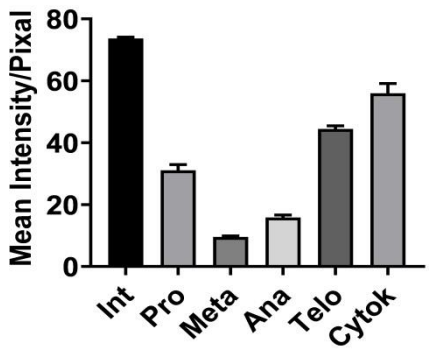
Mean Intensity/Pixal
80
60
40
20
0
Int
Pro
Meta
Ana
Telo
Cytok

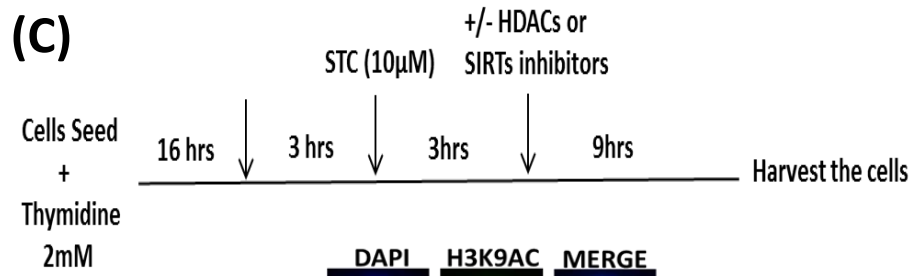
(C)
Cells Seed + Thymidine 2mM
16 hrs
3 hrs
STC (10µM)
3hrs
+/- HDACs or SIRTs inhibitors
9hrs
Harvest the cells

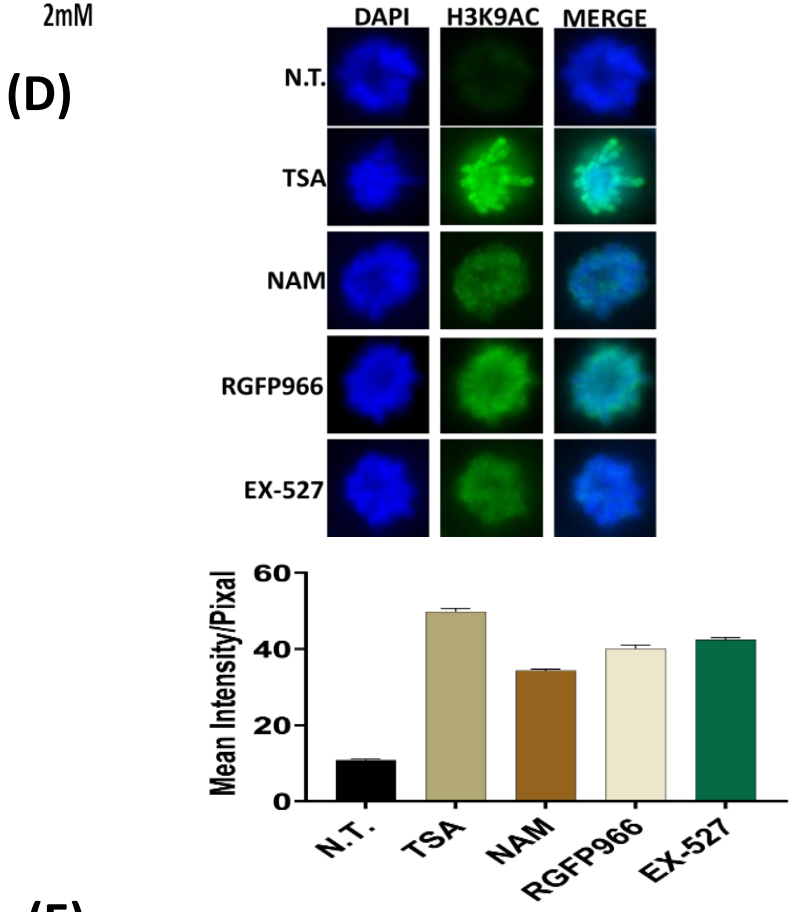
(D)
DAPI
H3K9AC
MERGE
N.T.
TSA
NAM
RGFP966
EX-527
Mean Intensity/Pixal
60
40
20
0
N.T.
TSA
NAM
RGFP966
EX-527

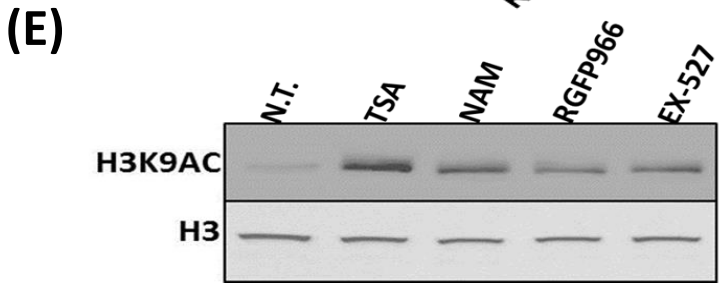
(E)
N.T.
TSA
NAM
RGFP966
EX-527
H3K9AC
H3

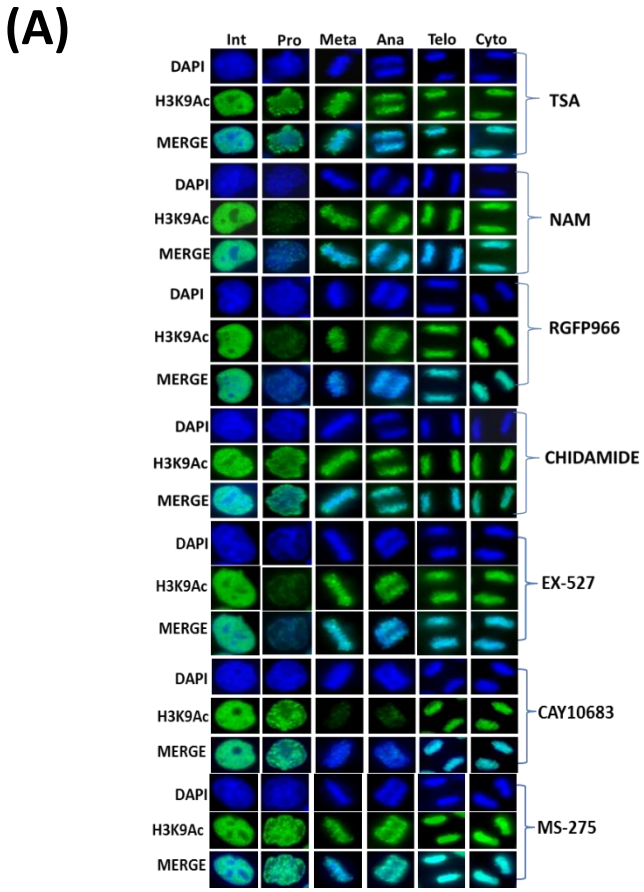
(A)
Int
Pro
Meta
Ana
Telo
Cyto
DAPI
H3K9Ac
MERGE
TSA
NAM
RGFP966
CHIDAMIDE
EX-527
CAY10683
MS-275

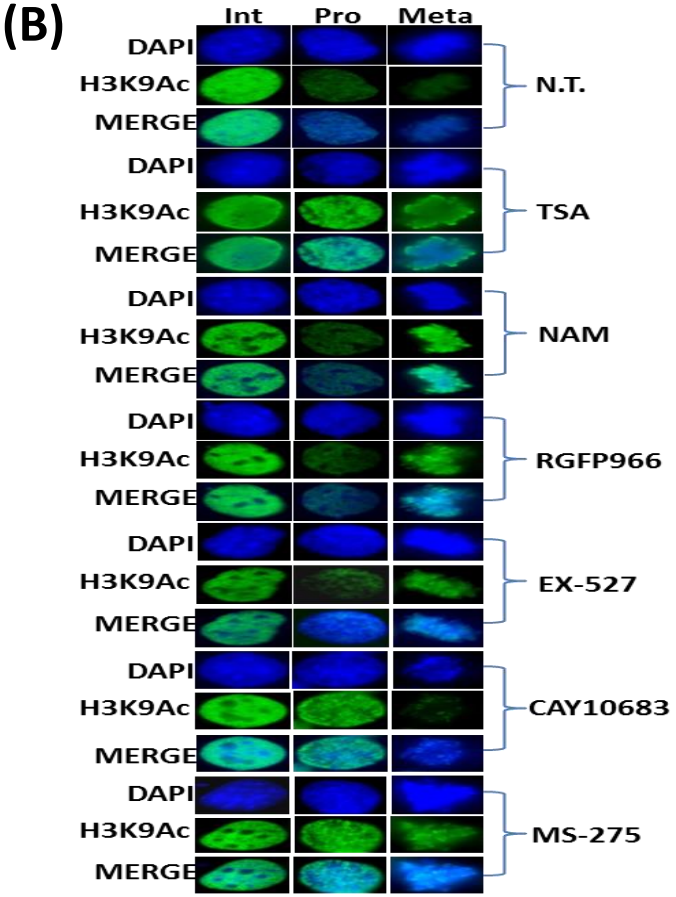
(B)
Int
Pro
Meta
DAPI
H3K9Ac
MERGE
N.T.
TSA
NAM
RGFP966
EX-527
CAY10683
MS-275

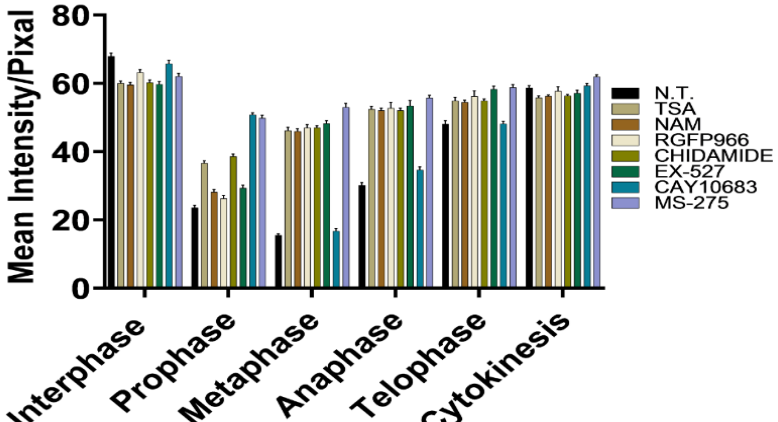
Mean Intensity/Pixal
80
60
40
20
0
Interphase
Prophase
Metaphase
Anaphase
Telophase
Cytokinesis
N.T.
TSA
NAM
RGFP966
CHIDAMIDE
EX-527
CAY10683
MS-275

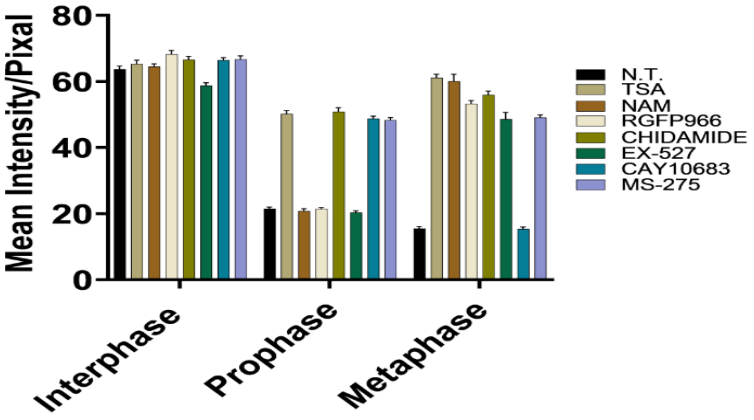
Mean Intensity/Pixal
80
60
40
20
0
Interphase
Prophase
Metaphase
N.T.
TSA
NAM
RGFP966
CHIDAMIDE
EX-527
CAY10683
MS-275

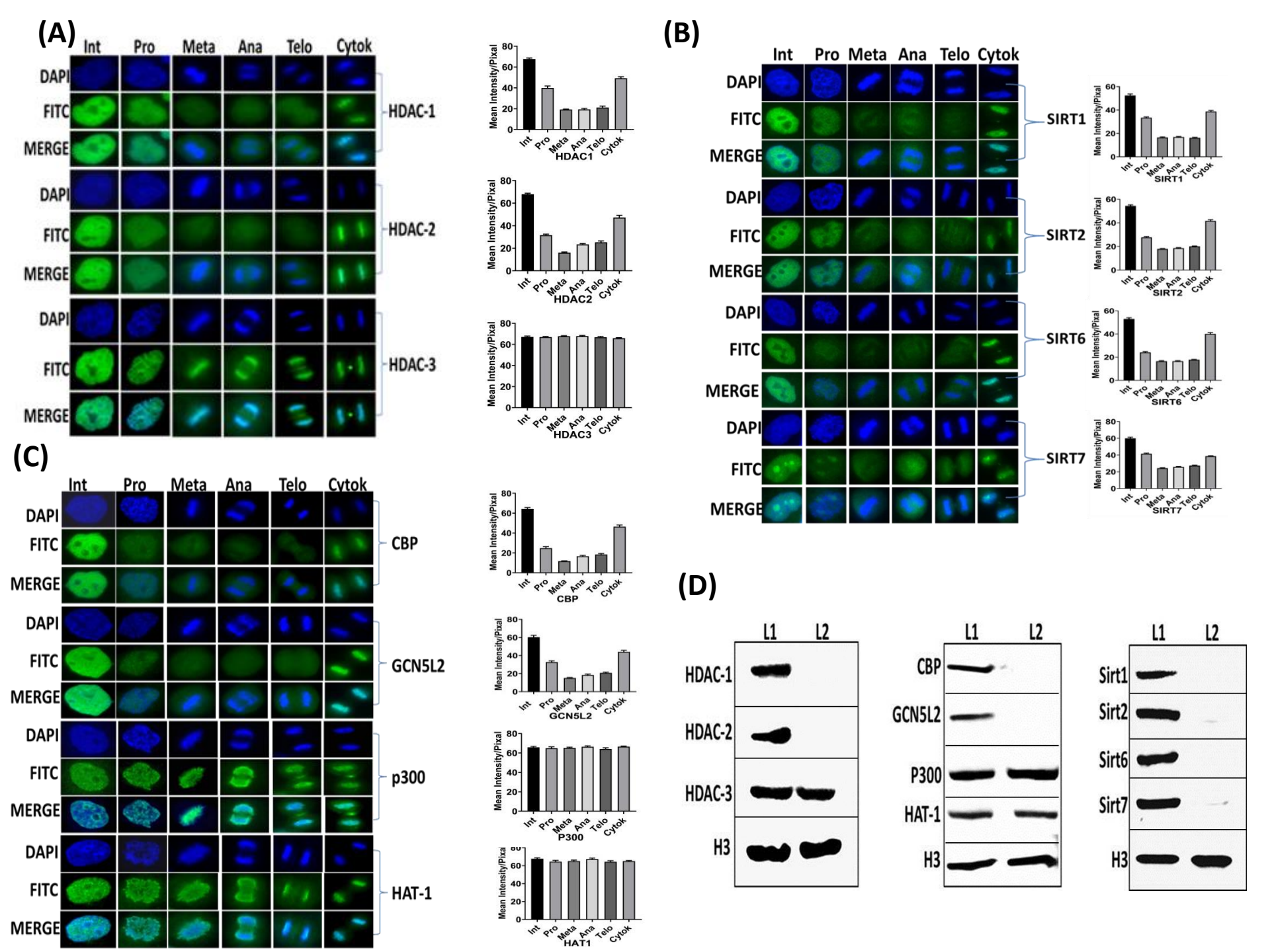
(A)
Int
Pro
Meta
Ana
Telo
Cytok
DAPI
FITC
MERGE
HDAC-1
HDAC-2
HDAC-3
Mean Intensity/Pixal
HDAC1
HDAC2
HDAC3
(B)
SIRT1
SIRT2
SIRT6
SIRT7
(C)
CBP
GCN5L2
p300
HAT-1
(D)
L1
L2
HDAC-1
HDAC-2
HDAC-3
H3
CBP
GCN5L2
P300
HAT-1
Sirt1
Sirt2
Sirt6
Sirt7

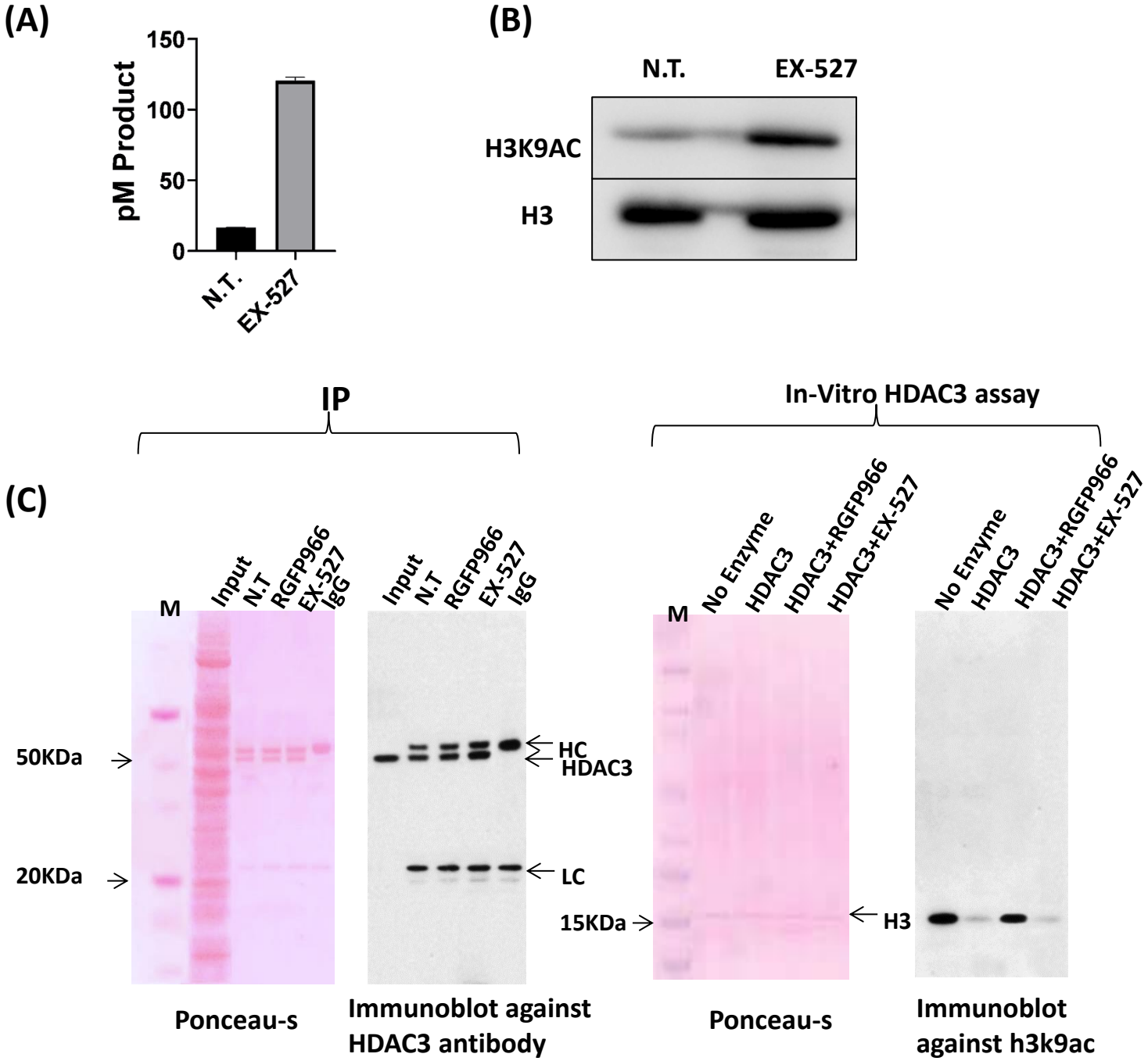
(A)
pM Product
150
100
50
0
N.T.
EX-527
(B)
N.T.
EX-527
H3K9AC
H3
IP
In-Vitro HDAC3 assay
(C)
M
Input
N.T
RGFP966
EX-527
IgG
Input
N.T
RGFP966
EX-527
IgG
M
No Enzyme
HDAC3
HDAC3+RGFP966
HDAC3+EX-527
No Enzyme
HDAC3
HDAC3+RGFP966
HDAC3+EX-527
50KDa
20KDa
HC
HDAC3
LC
15KDa
H3
Ponceau-s
Immunoblot against HDAC3 antibody
Ponceau-s
Immunoblot against h3k9ac

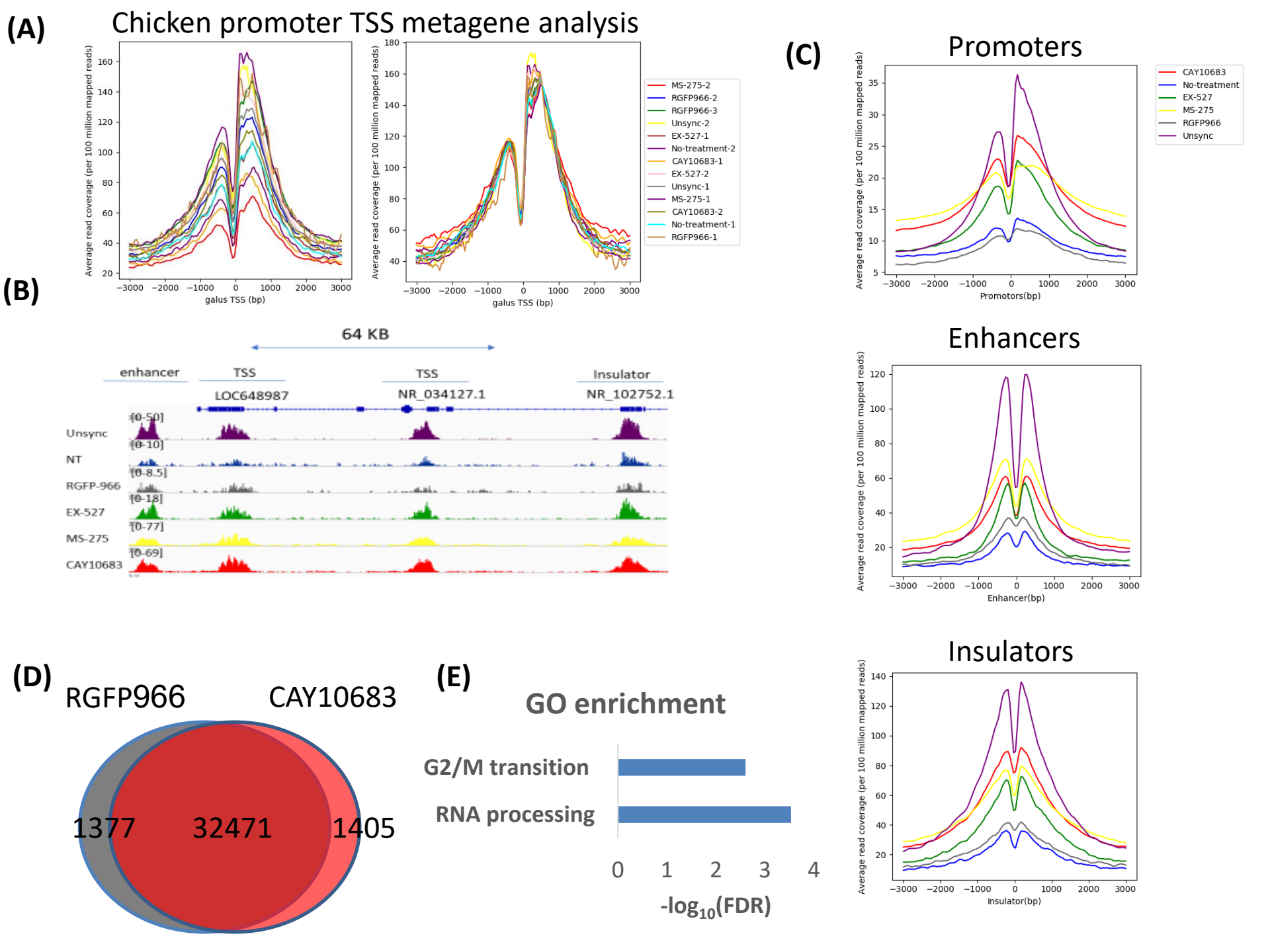
(A)
Chicken promoter TSS metagene analysis
Average read coverage (per 100 million mapped reads)
galus TSS (bp)
MS-275-2
RGFP966-2
RGFP966-3
Unsync-2
EX-527-1
No-treatment-2
CAY10683-1
EX-527-2
Unsync-1
MS-275-1
CAY10683-2
No-treatment-1
RGFP966-1
(B)
64 KB
enhancer
TSS
TSS
Insulator
LOC648987
NR_034127.1
NR_102752.1
Unsync
NT
RGFP-966
EX-527
MS-275
CAY10683
(C)
Promoters
Average read coverage (per 100 million mapped reads)
Promotors(bp)
CAY10683
No-treatment
EX-527
MS-275
RGFP966
Unsync
Enhancers
Average read coverage (per 100 million mapped reads)
Enhancer(bp)
Insulators
Average read coverage (per 100 million mapped reads)
Insulator(bp)
(D)
RGFP966
CAY10683
1377
32471
1405
(E)
GO enrichment
G2/M transition
RNA processing
-log10(FDR)